Twenty amino acids in the PA-X C-terminal affect the virulence of influenza A viruses

Huijie Gao [a†], Honglei Sun [a†], Lu Qi [a], Jinliang Wang [a], Xin Xiong [a], Yu Wang [a], Qiming He [a], Yang Lin [a], Weili Kong [a], Lai-Giea Seng [b], Juan Pu [a], Kin-Chow Chang [b], Jinhua Liu [a] and Yipeng Sun [a,#]

[a] Key Laboratory of Animal Epidemiology and Zoonosis, Ministry of Agriculture, College of Veterinary Medicine, China Agricultural University, Beijing, China

[b] School of Veterinary Medicine and Science, University of Nottingham, Sutton Bonington Campus, United Kingdom

Running title: The role of PA-X C-terminal on influenza viruses

[#]Corresponding author. Key Laboratory of Animal Epidemiology and Zoonosis, Ministry of Agriculture, College of Veterinary Medicine, China Agricultural University, No. 2 Yuanmingyuan West Road, Beijing 100193, China.

Tel: +86-10-62732982; Fax: +86-10-62732982; E-mail: sypcau@163.com

[†] Huijie Gao and Honglei Sun contributed equally to this work.

Word counts: Abstract: 250; Main text: 4233

Abstract

The PA-X protein of influenza A virus was recently found to have arisen from ribosomal frame-shift during PA translation. The X ORFs of PA-X of diverse influenza A viruses can be divided into two groups according to the protein length: full length PA-X (61 amino acids) and truncated PA-X (41 amino acids). A previous study reported that the truncation of PA-X may be associated with the adaptation and emergence of the influenza virus in host species. However, the role of the C-terminal 20 amino acids of PA-X in influenza A viruses is still unclear. In the present study, a variety of epidemiologically important influenza A virus strains, including 2009 pandemic H1N1 (pH1N1), a highly pathogenic avian influenza virus of the H5N1 subtype, and a lowly pathogenic avian H9N2 influenza virus, served as models of prevalent human and avian influenza viruses, respectively, to evaluate the impact of the C-terminal 20 amino acids of PA-X on viral replication and pathogenicity. For all tested viruses, those with full-length PA-X replicated more efficiently and caused more apoptosis in human lung cells than truncated ones. Viruses with full length PA-X were also more virulent and caused more severe inflammatory responses in mice than those with truncated PA-X. The C-terminal 20 amino acids of full-length PA-X accelerated nuclear accumulation of PA protein and enhanced polymerase activity of pH1N1, H5N1, and H9N2 viruses. The current study addresses the role of the C-terminal 20 amino acids of full length PA-X on the biological characteristics of influenza A viruses.

Importance

In nature, the PA-X proteins of many types of influenza A viruses can be divided into two groups according to the protein length: those with full-length PA-X and those with truncated PA-X. The role of the C-terminal 20 amino acids of PA-X in current epidemiologically important influenza A virus strains, including 2009 pandemic H1N1 (pH1N1), highly pathogenic avian influenza H5N1 and a lowly pathogenic avian H9N2 influenza viruses was demonstrated. Possible underlying processes including cell death, polymerase activity, and changes in PA protein function were also evaluated. The current findings suggest that the C-terminal 20 amino acids of PA-X enhanced replication and pathogenicity in A549 cells and mice for pH1N1, H5N1, and H9N2 viruses, which were associated with increased RNP polymerase activity, apoptosis, and elevated inflammatory response. The current study assesses the C-terminal 20 amino acids of PA-X as a virulence factor in the moderation of viral pathogenesis and pathogenicity.

Introduction

Influenza A virus (IAV) poses a significant threat to public health and causes considerable economic losses to the livestock industry. The magnitude of pathogenicity depends on virus and host. Infections range from asymptomatic to 100% lethal. The reasons for this disparity in pathogenesis are unclear because the molecular signatures of virulence of influenza viruses are not known. IAV is an enveloped negative-strand RNA virus, and its genome comprises eight viral RNA (vRNA) segments. The genome of the influenza virus may encode 10 viral proteins in total, PB2, PB1, PA, HA, NP, NA, M1, M2, NS1, and NS2 (1, 2). Additional novel proteins have been discovered as a second or third polypeptide made from PB1 and PA mRNA. Some of these proteins, such as PB1-F2 and PA-N155, are virulence factors for the influenza virus (3-5). Recently, it has been demonstrated that segment 3 of the influenza A virus encodes not only the PA protein but also an additional novel protein, PA-X, translated as a +1 frameshift open reading frame (X-ORF) extension of a growing PA polypeptide (6). PA-X inhibits host protein synthesis and hinders the host antiviral response (6, 7). Interestingly, PA-X in the 1918 pandemic H1N1 virus reduces viral pathogenicity in mice (6).

PA-X is a fusion protein that comprises the N-terminal domain of PA (191 amino acids) and the C-terminal domain X. Comprehensive genetic analysis showed that the X ORFs of diverse influenza A viruses can be divided into two groups according to the protein length (8). Avian, equine, and human seasonal H3N2 and H1N1 influenza viruses express a full-length PA-X protein with 61 amino acids in the X domain. By contrast, some influenza A viruses, including human 2009 pandemic H1N1 (pH1N1), canine, and certain swine influenza viruses possess a TGG (Trp) to TAG (stop codon) mutation at codon 42 in the X-ORF. This mutation produces a truncated PA-X protein with 41 amino acids in the X domain. It remains unclear whether the C-terminal 20 amino acids of PA-X influence the biological characteristics of the virus.

pH1N1 influenza virus infection was the first pandemic of the 21st century and is still circulating in human and pig populations (9-11). The highly pathogenic H5N1 avian influenza viruses have undergone widespread geographic expansion among wild

and domestic birds. They are deadly pathogens in chickens and humans and may cause a future influenza pandemic (12-14). H9N2 influenza viruses are endemic in many terrestrial avian species in Asia and occasionally transmit to mammalian species including humans and pigs (15-19). The PA-X ORFs of pH1N1viruses are the truncated 41 amino acids in the X domain, and H5N1 and H9N2 avian influenza viruses express full-length PA-X with 61 amino acids in the X domain (Fig. 1A). To understand the role of the C-terminal 20 amino acids in the of PA-X in these influenza viruses, the effects of the full length and truncated forms of pH1N1, H5N1, and H9N2 PA-X on polymerase activity, viral replication, and pathogenicity were evaluated in mammalian cells and mice. Viruses with full-length PA-X here showed higher polymerase activity, replication, and pathogenicity than viruses with truncated PA-X in the indicated three strains.

Results

Generation of full-length PA-X pH1N1 and truncated PA-X H5N1 and H9N2 viruses

To assess the function of the C-terminal 20 amino acids of PA-X, sets of A/Beijing/16/2009 (BJ/09, pH1N1), A/Anhui/1/2005 (AH/05, H5N1) and A/chicken/Hebei/LC/2008 (HB/08, H9N2) viruses (full-length and truncated PA-X) were generated using reverse genetics. A698G of PA-X ORF in pH1N1-61X and G698A of PA-X ORF in H5N1-41X and H9N2-41X viruses did not affect the PA ORF (Fig. 1A). Western blotting was performed to demonstrate the PA-X expression in all indicated viruses infected MDCK cells (Fig. 1B). PA-X was detected in pH1N1-41X (WT), pH1N1-61X, H5N1-61X (WT), H5N1-41X, H9N2-61X (WT), and H9N2-41X infected cells.

The C-terminal 20 amino acids of full-length PA-X played a role in viral replication and apoptosis of influenza viruses in human lung cells

Six viruses were used to infect MDCK and A549 cells at an MOI of 0.01, and the supernatants were collected and titrated at 12, 24, 36, 48, 60, 72, 84, and 96 hpi. There was no significant difference in viral output from MDCK cells between two forms of pH1N1, H5N1, and H9N2 viruses (Fig. 2A). However, with A549 cells, the mutant

virus with full-length PA-X, pH1N1-61X, showed higher levels than those with truncated PA-X [pH1N1-41X (WT)] from 48 hpi ($P < 0.05$) (Fig. 2B). H5N1-61X (WT) with full length PA-X showed higher replication levels than H5N1-41X with truncated PA-X at 84 and 96 hpi ($P < 0.05$). Full length PA-X virus, H9N2-61X (WT), produced higher virus levels than with truncated PA-X, H9N2-41X, at 24, 36, and 48 hpi ($P < 0.05$). The data from A549 cells showed that pH1N1, H5N1, and H9N2 viruses with full length PA-X appeared to replicate more efficiently than corresponding viruses with truncated PA-X.

Influenza viruses induce apoptosis and necrosis in infected cells, so causing cellular and organ damage (20, 21). It has been previously shown that several viral proteins (NA, M1, NS1, and PB1-F2) promote apoptosis in cells (22-26). To evaluate the effect of the C-terminal 20 amino acids of full length PA-X on cell death, A549 cells were infected with a panel of recombinant viruses at 1.0 MOI for 12 h. Evaluation of apoptosis and necrosis by flow cytometry for annexinV^+ and PI^+ cells revealed that pH1N1-61X virus caused more apoptosis (22.94%) than pH1N1-41X (WT) virus (13.25%) ($P < 0.05$) (Fig. 2C). Similarly, H5N1-61X (WT) virus produced more apoptotic cells (27.5%) than H5N1-41X virus (17.97%) and H9N2-41X virus produced fewer apoptotic cells (11.82%) than H9N2-61X (WT) virus (15.17%) ($P < 0.05$). These results indicated that viruses with full length PA-X induced an increase in apoptosis in A549 cells than those with truncated PA-X for pH1N1, H5N1 and H9N2 viruses.

Viruses with full-length PA-X were more virulent than those with truncated PA-X in mice

To assess the pathogenicity of PA-X mutants, six-week-old BALB/c mice were intranasally inoculated with each virus. Clinical signs, mortality, and weight loss were monitored over 14 days. Virus-infected mice were humanely killed at 3, 5, and 7 days post-infection (dpi), and lungs were collected for virus titration. For pH1N1 mutants, survival curves for the 10^5 $TCID_{50}$ infection dose clearly showed that pH1N1-61X had a higher pathogenicity than pH1N1-41X (WT). pH1N1-61X had 100% mortality by 8 dpi; pH1N1-41X (WT) caused no deaths (Fig. 3A). The loss of body weight due

150 to pH1N1-61X was greater than that attributed to pH1N1-41X (WT) (Fig. 3B). The
151 pathogenicity of these viruses was further demonstrated by histopathology of lung
152 tissues collected at 5 dpi. As shown in Fig. 5A, pH1N1-61X caused more severe
153 lesions than pH1N1-41X (WT) mutants, exhibiting extensive alveolar damage and
154 cellular infiltration. Moderate interstitial pneumonia was observed in pH1N1-41X
155 (WT)-infected lungs. pH1N1-61X showed higher viral replication in the lung than
156 pH1N1-41X (WT) at 5 and 7 dpi (Fig. 4B).

157 In H5N1 mutants, H5N1-41X ($MLD_{50} = 10^{2.75}$ $TCID_{50}$) was attenuated in mice than
158 H5N1-61X (WT) of which MLD_{50} was $10^{2.25}$ $TCID_{50}$, and body weight loss of
159 H5N1-41X-infected mice were less than H5N1-61X (WT) after inoculation at 10^2
160 $TCID_{50}$ or 10^3 $TCID_{50}$ (Fig. 3D & F). The survival curves showed that H5N1-61X
161 (WT) was more pathogenic than H5N1-41X. H5N1-61X had 100% mortality by 9 dpi;
162 H5N1-41X caused 66.6% mortality after inoculation at 10^3 $TCID_{50}$. H5N1-61X (WT)
163 showed greater pathogenicity than H5N1-41X, with 33.3% mortality by 12 dpi;
164 H5N1-41X caused no deaths after inoculation at 10^2 $TCID_{50}$ (Fig. 3C & E). The titers
165 of H5N1-41X in lungs were significantly lower than those of H5N1-61X (WT) at 3
166 and 7 dpi ($P < 0.05$) in mice that had been inoculated with 10^3 $TCID_{50}$ of each H5N1
167 mutant (Fig. 4C). Both H5N1-61X (WT) and H5N1-41X were detected in the brains
168 and blood of mice, but H5N1-61X (WT) showed a higher replication level in the brain
169 than H5N1-41X at 5 dpi (Fig. 5D). Mice infected with H5N1-61X (WT) showed more
170 severe lesions than those infected with H5N1-41X. These infections were
171 characterized by interstitial edema, thickening of the alveolar walls, and cellular
172 infiltration (Fig. 4A).

173 As indicated in the survival curves of mice infected with H9N2 mutants at 10^6
174 $TCID_{50}$, H9N2-41X infection resulted in no deaths, but H9N2-61X (WT) infection
175 had 33.3% mortality (Fig. 3G). The maximum weight loss from H9N2-61X (WT) and
176 H9N2-41X infection was 12% and 5%, respectively (Fig. 3H). Lungs infected with
177 H9N2-41X virus appeared almost normal, but mild pathological changes were
178 detected in the H9N2-61X (WT) group. Some vessel walls were surrounded by
179 inflammatory cells and epithelial erosion of bronchial lining (Fig. 4A). The viral titers

of lungs infected with H9N2-41X were lower than those of those infected with H9N2-61X (WT) at 3, 5, and 7 dpi ($P < 0.05$) (Fig. 4E). This was consistent with the observed pathology.

Collectively, these results indicated that pH1N1, H5N1, and H9N2 viruses with full-length PA-X were more pathogenic than those with truncated PA-X.

Viruses with full-length PA-X caused more severe inflammatory responses in mice than those with truncated PA-X

Severe influenza virus infection in human and animal models is associated with abnormally elevated pulmonary pro-inflammatory cytokine and chemokine expression (27-30). To assess the effect of the C-terminal 20 amino acids of PA-X on host inflammatory response, the protein levels of seven cytokines and chemokines in the lungs of infected mice were measured at 3 and 5 dpi.

Mice infected with pH1N1-61X containing full-length PA-X virus exhibited higher titers of IFN-γ, IL-1β, IL-6, KC, TNF-α, and MIP-1α than those with pH1N1-41X (WT) at 3 and 5 dpi ($P < 0.05$) (Fig. 5A). Mice infected with H5N1-61X with full-length PA-X showed higher levels of IFN-γ, IL-6, KC, TNF-α, and MIP-1α than H5N1-41X expressing truncated PA-X at 3 or 5 dpi ($P < 0.05$) (Fig. 5B). For H9N2 mutants, all the chemokine and cytokine levels of H9N2-61X (WT) were higher than that of H9N2-41X at 3 and 5 dpi ($P < 0.05$) (Fig. 5C).

These results showed that infection with pH1N1, H5N1, and H9N2 viruses carrying full-length PA-X tended to elicit a more severe inflammatory response than infection with truncated PA-X viruses.

Full-length PA-X proteins exhibited higher polymerase activity than their respective truncated forms

The viral ribonucleoprotein (RNP) complex has been shown to be correlated with viral replication and pathogenicity (31, 32). An influenza virus mini-genome assay was performed on 293T cells to determine the effect of the C-terminal 20 amino acids of PA-X on viral polymerase activity (33). The RNP polymerase activity from pH1N1-61X expressing full length PA-X protein was 50% more pronounced than that of pH1N1-41X (WT) ($P < 0.05$) (Fig. 6A). H5N1-41X showed 15% less RNP

polymerase activity than H5N1-61X (WT) ($P < 0.05$) (Fig. 6B). For the H9N2 virus constructs, H9N2-61X (WT) RNP activity was 25% greater than that of H9N2-41X ($P < 0.05$) (Fig. 6C). These results indicated full-length PA-X proteins had more polymerase activity than their respective truncated forms of PA-X in the pH1N1, H5N1, and H9N2 viruses.

Protein lysates derived from 293T cells transfected with RNP plasmids were analyzed by Western blotting. Synonymous mutations in PA genes did not affect PA protein expression for pH1N1, H5N1, or H9N2 viruses (Fig. 6D). In summary, the more pronounced RNP polymerase activity of full-length PA-X in pH1N1, H5N1, and H9N2 viruses was found not to be due to the differences in expression of the PA protein.

The C-terminal 20 amino acids of full length PA-X increased the nuclear localization of PA protein and suppressed non-viral protein expression

Accumulation of PA protein in the nucleus was found to be correlated with the pathogenicity of influenza viruses in mice (34-36). The role of the C-terminal 20 amino acids of PA-X on PA protein accumulation in the nuclei of infected cells was evaluated. A549 cells were infected with full-length and truncated PA-X pH1N1, H5N1, and H9N2 viruses at 2.0 MOI. The extension of cytoplasmic accumulation of PA into the nucleus was accelerated such that, at 6 hpi, more cells were infected with pH1N1 or H5N1 virus with full length PA-X than with truncated. At 10 hpi, more cells infected with H9N2 virus with full-length PA-X showed nuclear presence of PA than cells infected with the corresponding virus with truncated PA-X (Fig. 7).

The PA gene plays a major role in the suppression of host protein synthesis, and this role involves PA-X (6, 37). In order to determine the role of the C-terminal 20 amino acids of PA-X in the suppression of host protein synthesis, the PA activity of full-length PA-X was compared to that of truncated PA-X in pH1N1, H5N1, and H9N2 viruses. Specifically the suppression of non-viral protein synthesis was observed in 293T cells over the course of 24 h using co-transfection of pEGFP and corresponding PA plasmids. There was significantly less eGFP expression in the presence of H1N1-61X than in the presence of H1N1-41X (WT), and there was

significantly more in the presence of H5N1-41X PA and H9N2-41X PA than in the presence of H5N1-61X (WT) PA or H9N2-61X (WT) PA respectively (Fig. 8). In this way, full-length PA-X was found to speed up nuclear accumulation of PA protein and render PA more effective in suppressing non-viral protein expression.

Discussion

The polymerase activity, viral replication, and pathogenicity of the full length and truncated forms of PA-X were evaluated in pH1N1, H5N1, and H9N2 viruses. In all three strains viruses with full length PA-X showed more polymerase activity, replication, and pathogenicity than those with truncated PA-X.

Two forms of PA-X proteins were observed in influenza A viruses: the full-length form (61 amino acids in X-ORF) and the truncated form (41 amino acids in X-ORF) (6, 8). The two forms of PA-X in pH1N1, H5N1, and H9N2 viruses showed no significant difference in virus replication in MDCK cells. Jagger *et al.* reported similar results in MDCK cells but found no difference in single or multicycle growth kinetics of the 1918 H1N1 PA-X-deficient virus and wild type (6). However, it was here found that pH1N1, H5N1, and H9N2 viruses with full-length PA-X showed higher replication levels and caused more apoptosis in A549 cells than those with truncated PA-X. Results also showed that full-length PA-X exhibited more pathogenicity (mortality and lung pathology) than truncated PA-X in corresponding viruses. These results suggest that the mutational switch from truncated to full-length PA-X could indicate increased pathogenicity. Attention should be paid to the switch from truncated PA-X to the full-length form. Although 2009 pandemic H1N1 virus strains with full-length PA-X do not appear in nature at present, the possibility of pH1N1 acquiring full-length PA-X proteins by mutation cannot be excluded.

Results showed that pH1N1, H5N1, and H9N2 viruses with full-length PA-X had more polymerase activity than those with truncated PA-X. This was consistent with their pathogenicity. The full-length and truncated PA-X differed in the presence of 20 amino acids near the C-terminal. It is here suggested that the C-terminal 20 amino acids of the full length PA-X contribute to viral polymerase activity and pathogenicity.

There is some evidence that pathogenicity is associated with inflammatory

responses. Cytokine and chemokine responses, including those of IL-1β, IFN-γ, TNF-α, MIP-1α, IL-6, MIP-2, MCP-1, KC, and IL-1α, were found to be associated with the recruitment of macrophages and neutrophils to the infected lungs, which caused acute lung inflammation (30). Jagger *et al.* found that PA-X down-regulated the immune response and inflammation during infection with the 1918 pandemic virus (6). In the current study, in pH1N1, H5N1, and H9N2 viruses, full-length PA-X tended to elicit more severe pro-inflammatory responses and more pathogenicity than truncated PA-X. It is here suggested that full length PA-X could promote host inflammatory response.

The C-terminal 20 amino acids of full-length PA-X affected nuclear accumulation of PA protein and support the suppressive role of PA protein on host protein synthesis. Previous studies have reported that the level of polymerase accumulation in the nuclei of infected cells is correlated with the virulence of influenza virus (34, 38). The present study showed that the C-terminal 20 amino acids of full-length PA-X accelerated nuclear accumulation of the PA protein in A549 cells. The increased nuclear accumulation of PA was consistent with the increased virulence of pH1N1, H5N1, and H9N2 viruses. In addition, PA proteins with full-length PA-X were more effective in suppressing host protein expression, suggesting that the C-terminal 20 amino acids of full-length PA-X play a role in the suppression of host protein synthesis.

Under natural conditions, there are changes in the length of PA-X protein of influenza A viruses. For example, truncation of PA-X occurs when avian and equine influenza viruses are introduced to canines, and the classic swine H1N1 viruses with the truncated form of PA-X (a cluster of viruses sampled between 1985 and 2009) were directly derived from those with full-length PA-X (a group of generally older 1930 to 2006 classic swine H1N1 viruses) (8). For these reasons, epidemiological surveys should pay attention to viruses full-length PA-X, especially pH1N1 viruses.

Materials and methods

Ethics statement

All animal work was approved by the Beijing Association for Science and Technology (approval ID SYXK [Beijing] 2007-0023) and conducted in strict

accordance with the Beijing Laboratory Animal Welfare and Ethics guidelines, as issued by the Beijing Administration Committee of Laboratory Animals, and in accordance with the China Agricultural University (CAU) Institutional Animal Care and Use Committee guidelines approved by the Animal Welfare Committee of CAU.

Viruses and cells

A/Beijing/16/2009 (BJ/09, pH1N1), A/Anhui/1/2005 (AH/05, H5N1), and A/chicken/Hebei/LC/2008 (HB/08, H9N2) viruses were described previously (39, 40). Human embryonic kidney cells (293T), Madin-Darby canine kidney cells (MDCK), and human pulmonary adenocarcinoma cells (A549) were maintained in Dulbecco's modified Eagle's medium (DMEM; Life Technologies, Foster City, CA, U.S.) supplemented with 10% fetal bovine serum (FBS; Life Technologies), 100 units/ml of penicillin and 100 g/ml of streptomycin.

Generation of recombinant viruses by reverse genetics

All eight gene segments were amplified by reverse transcription-PCR (RT-PCR) from BJ/09, AH/05, and HB/08 viruses and cloned into the dual-promoter plasmid, pHW2000. The mutations were introduced into the PA gene using a Site-directed QuikChange Mutagenesis Kit according to the manufacturer's instructions (Agilent, Santa Clara, CA, U.S.). PCR primer sequences are available upon request. pH1N1 with full-length PA-X (61 amino acids), pH1N1-61X, had a stop (UAG)-to-tryptophan codon (UGG) substitution at position 42 in X ORF (stop42W) without changing the PA ORF (Fig. 1B). H5N1 and H9N2 viruses with truncated PA-X (41 amino acids), H5N1-41X and H9N2-41X, which had a tryptophan (UGG)-to-stop codon (UAG) substitution at 42 site in X ORF (W42stop) without altering the PA ORF. Rescued viruses were detected using hemagglutination assays. Viral RNA was extracted and analyzed by RT-PCR, and each viral segment was sequenced to confirm sequence identity.

All experiments with live viruses and transfectants generated by reverse genetics were performed in a biosafety level 3 containment laboratory approved by the Ministry of Agriculture of the People's Republic of China.

Viral titration and replication kinetics

330 The 50% tissue culture infectious dose ($TCID_{50}$) was determined in MDCK cells
331 using 10-fold serially diluted virus inoculated at 37°C and cultured for 72 h. The
332 $TCID_{50}$ values were calculated using the method first described by Reed and Muench
333 (41).
334 MDCK and A549 cells were infected with virus at a multiplicity of infection
335 (MOI) of 0.01. Supernatants of the infected MDCK cells were harvested at 6, 12, 24,
336 36, 48, 60, 72, and 84 h post infection (hpi). Supernatants of the infected A549 cells
337 were harvested at 12, 24, 36, 48, 60, 72, 84, and 96 hpi. Viral titers were determined
338 in MDCK cells from the $TCID_{50}$. Three independent experiments were performed.
339 **Mouse infection**
340 Fifteen mice (six week-old female BALB/c; Vital River Laboratory, Beijing, China)
341 per group were anesthetized with Zoletil (tiletamine-zolazepam; Virbac S.A., Carros,
342 France; 20 μg/g) and inoculated intranasally with 50 μl of 10^5 $TCID_{50}$ of pH1N1 or
343 10^2 or 10^3 $TCID_{50}$ of H5N1 or 10^6 $TCID_{50}$ of H9N2, diluted in phosphate-buffered
344 saline (PBS). All mice were monitored daily for 14 days; mice that lost 30% of their
345 original body weight were humanely euthanized. Three mice were euthanized 3, 5,
346 and 7 days post infection (dpi) for determination of lung virus titers, histology, and
347 cytokine levels. Lungs were collected and homogenized in 1 ml of cold PBS. Virus
348 titers were determined by $TCID_{50}$. The 50% minimum lethal dose (MLD_{50}) values
349 were determined by intranasally inoculating groups of three mice with 10-fold
350 dilutions of virus and were calculated by the method of Reed and Muench (41).
351 **Histopathology**
352 At 5 dpi, a portion of lung from each euthanized mouse was fixed in 10%
353 phosphate-buffered formalin and processed for paraffin embedding. Each 5 μm
354 section was stained with hematoxylin and eosin (H&E) and examined for
355 histopathological changes. Images were captured with a Zeiss Axioplan 2IE
356 epifluorescence microscope.
357 **Polymerase activity assays**
358 RNP Minigenome Luciferase Assay. Four expression plasmids housing PB2, PB1,
359 PA, and NP (125 ng each) from BJ/09, AH/05 and HB08 viruses [pH1N1-41X (WT),

pH1N1-61X, H5N1-61X (WT), H5N1-41X, H9N2-61X (WT), and H9N2-41X)] were cloned based on the eukaryotic expression vector pcDNA3.1 and co-transfected into 293T cells with fire-fly luciferase reporter plasmid pYH-NS1-Luci (10 ng) and internal control plasmid expressing renilla luciferase (2.5 ng). The assay was performed at 37°C. At 24 hpi, cell lysate was prepared using a Dual-Luciferase Reporter Assay System (Promega) and luciferase activity was measured using a GloMax 96 microplate luminometer (Promega).

Quantification of cytokine and chemokine protein levels in mouse lungs

Levels of cytokines and chemokines, including interleukin-1 beta (IL-1β), interleukin-6 (IL-6), mouse interleukin-8 (IL-8), monocyte chemotactic protein 1 (MCP-1), macrophage inflammatory protein 1 alpha (MIP-1α), tumor necrosis factor alpha (TNF-α), and interferon γ (IFN-γ) in the lung were determined using a cytometric bead array method (BD Cytometric BEAD Array Mouse Inflammation Kit; BD Bioscience, San Diego, CA, U.S.). Briefly, 50 μl mouse inflammation capture bead suspension and 50 μl detection reagent were added to an equal amount of sample and incubated in the dark for 2 h at room temperature. Samples were later washed with 1 ml wash buffer and then centrifuged at 200 × *g* at room temperature for 5 min. Supernatants were discarded and 300 μl wash buffer was added. Samples were analyzed on a BD FACS Array bioanalyzer (BD Bioscience). Data were analyzed using BD CBA Software (BD Bioscience). Chemokine and cytokine levels were recorded as pg/ml in the homogenate.

Cell death assays

Virus infection assays were conducted in 6-well plates. Cells were seeded at a density of 1×10^6 cells/well for overnight in infection media (cell growth media with 1% bovine serum albumin (BSA) was used in place of FCS). Cells were then infected with virus at 1.0 MOI for 12 h. Cells from the supernatant and monolayers were then harvested, washed, and stained with APC labeled annexin and propidium iodide (PI) (Becton Dickinson, San Jose, CA, U.S.) for 20 min. After a final wash step, cells were resuspended in 100 μl FACs wash buffer (PBS containing 3% BSA and 0.01% sodium azide) and analyzed on the FACs Calibur (BD Biosciences) and BD CellQuest Pro

software (version 5.2.1, BD Biosciences). Cell death (apoptosis and necrosis) was defined as annexin-V^+ and PI^+, while apoptotic cells were annexin-V^+ only. Viable cells were considered neither annexin-V nor PI positive.

Western blotting

Total cell protein lysates were extracted from transfected 293T cells and infected MDCK cells with CA630 lysis buffer (150 mM NaCl, 1% CA630 detergent, 50 mM Tris base [pH 8.0]). Cellular proteins were separated by 12% sodium dodecyl sulfate-polyacrylamide gel electrophoresis (SDS-PAGE) and transferred to a polyvinylidene difluoride (PVDF) membrane (Amersham Biosciences, Freiburg, Germany). Each PVDF membrane was blocked with 0.1% Tween 20 and 5% nonfat dry milk in Tris-buffered saline and subsequently incubated with a primary antibody. Primary antibodies were specific to influenza A virus PA (1:3000, GeneTex, Alton Pkwy Irvine, U.S.), influenza A virus NP (diluted 1:3000, GeneTex U.S.), influenza A virus PA-X (diluted 1:2000, was provided by Dr. Xiufan Liu of YangZhou University, China). Secondary antibodies used here included horse radish peroxidase (HRP)-conjugated anti-mouse antibody or HRP-conjugated anti-rabbit antibody (diluted 1:10,000 Jackson ImmunoResearch, West Grove, U.S.), as appropriate. HRP presence was detected using a Western Lightning Chemiluminescence Kit in accordance with the manufacturer's protocol (Amersham Pharmacia, Freiburg, Germany).

Immunofluorescence

A549 cells were grown on glass-bottom dishes and infected at 2.0 MOI with the indicated virus. At specified points in time after infection, the cells were fixed with PBS containing 4% paraformaldehyde for 20 min and permeabilized with PBS containing 0.5% Triton X-100 for 30 min. After blocking with 5% BSA in PBS, the cells were incubated with rabbit antisera against PA (diluted 1:400 GeneTex U.S.) at room temperature for 2 h. The cells were then washed three times with PBS and incubated for 1 h with fluorescein isothiocyanate (FITC)-coupled goat anti-rabbit secondary antibodies (diluted 1:100, Jackson ImmunoResearch, U.S.). The cells were subsequently washed three times with PBS and incubated with 4′,

6-diamidino-2-phenylindole (DAPI) for 10 min. Cells were imaged with a laser scanning confocal microscope (Leica). Localization of PA protein in the nucleus was determined by counting infected cells with nuclear presence of PA (n=100). The results shown represent three independent experiments.

Statistical analysis

The statistical analyses were performed using GraphPad Prism Software Version 5.00 (GraphPad Software Inc., San Diego, CA, U.S.). Comparison between two forms of treatment involved two-tailed Student's t-test; multiple comparisons were carried out using two-way analysis of variance (ANOVA) considering time and virus as factors. Differences were considered statistically significant at $P < 0.05$. The data are reported as the mean ± standard deviation (SD).

Acknowledgments

This work was supported by the National Natural Science Foundation of China (No. 31302102 and No. 31430086), the National Basic Research Program (973 Program) (No. 2011CB504702), a grant from the Chang Jiang Scholars Program, and a Biotechnology and Biological Sciences Research Council (UK) China Partnering Award.

References

1. **Palese P.** 1977. The genes of influenza virus. Cell **10**:1.
2. **Lamb R.** 1983. The influenza virus RNA segments and their encoded proteins, In: Palese P, Kingsbury DW, eds. Genetics of influenza viruses. New York: Springer-Verlag.
3. **Chen W, Calvo PA, Malide D, Gibbs J, Schubert U, Bacik I, Basta S, O'Neill R, Schickli J, Palese P.** 2001. A novel influenza A virus mitochondrial protein that induces cell death. Nat. Med. **7**:1306-1312.
4. **Wise HM, Foeglein A, Sun J, Dalton RM, Patel S, Howard W, Anderson EC, Barclay WS, Digard P.** 2009. A complicated message: Identification of a novel PB1-related protein translated from influenza A virus segment 2 mRNA. J. Virol. **83**:8021-8031.
5. **Muramoto Y, Noda T, Kawakami E, Akkina R, Kawaoka Y.** 2013. Identification of novel influenza A virus proteins translated from PA mRNA. J. Virol. **87**:2455-2462.

6. **Jagger B, Wise H, Kash J, Walters K-A, Wills N, Xiao Y-L, Dunfee R, Schwartzman L, Ozinsky A, Bell G.** 2012. An overlapping protein-coding region in influenza A virus segment 3 modulates the host response. Science **337**:199-204.
7. **Desmet EA, Bussey KA, Stone R, Takimoto T.** 2013. Identification of the N-terminal domain of the influenza virus PA responsible for the suppression of host protein synthesis. J. Virol. **87**:3108-3118.
8. **Shi M, Jagger BW, Wise HM, Digard P, Holmes EC, Taubenberger JK.** 2012. Evolutionary conservation of the PA-X open reading frame in segment 3 of influenza A virus. J. Virol. **86**:12411-12413.
9. **Trifonov V, Khiabanian H, Rabadan R.** 2009. Geographic dependence, surveillance, and origins of the 2009 influenza A (H1N1) virus. N. Engl. J. Med. **361**:115-119.
10. **Smith GJ, Vijaykrishna D, Bahl J, Lycett SJ, Worobey M, Pybus OG, Ma SK, Cheung CL, Raghwani J, Bhatt S, Peiris JS, Guan Y, Rambaut A.** 2009. Origins and evolutionary genomics of the 2009 swine-origin H1N1 influenza A epidemic. Nature **459**:1122-1125.
11. **Neumann G, Noda T, Kawaoka Y.** 2009. Emergence and pandemic potential of swine-origin H1N1 influenza virus. Nature **459**:931-939.
12. **Duan L, Bahl J, Smith G, Wang J, Vijaykrishna D, Zhang L, Zhang J, Li K, Fan X, Cheung C.** 2008. The development and genetic diversity of H5N1 influenza virus in China, 1996–2006. Virology **380**:243-254.
13. **Webster RG, Govorkova EA.** 2006. H5N1 influenza—continuing evolution and spread. N. Engl. J. Med. **355**:2174-2177.
14. **Xu X, Subbarao K, Cox NJ, Guo Y.** 1999. Genetic characterization of the pathogenic influenza A/Goose/Guangdong/1/96 (H5N1) virus: similarity of its hemagglutinin gene to those of H5N1 viruses from the 1997 outbreaks in Hong Kong. Virology **261**:15-19.
15. **Sun Y, Pu J, Jiang Z, Guan T, Xia Y, Xu Q, Liu L, Ma B, Tian F, Brown EG, Liu J.** 2010. Genotypic evolution and antigenic drift of H9N2 influenza viruses in China from 1994 to 2008. Vet. Microbiol. **146**:215-225.
16. **Xu KM, Smith GJ, Bahl J, Duan L, Tai H, Vijaykrishna D, Wang J, Zhang JX, Li KS, Fan XH, Webster RG, Chen H, Peiris JS, Guan Y.** 2007. The genesis and evolution of H9N2 influenza viruses in poultry from southern China, 2000 to 2005. J. Virol. **81**:10389-10401.
17. **Abolnik C, Gerdes GH, Sinclair M, Ganzevoort BW, Kitching JP, Burger CE, Romito M, Dreyer M, Swanepoel S, Cumming GS, Olivier AJ.** 2010. Phylogenetic analysis of influenza A viruses (H6N8, H1N8, H4N2, H9N2, H10N7) isolated from wild birds, ducks, and ostriches in South Africa from 2007 to 2009. Avian. Dis. **54**:313-322.
18. **Cong YL, Pu J, Liu QF, Wang S, Zhang GZ, Zhang XL, Fan WX, Brown EG, Liu JH.** 2007. Antigenic and genetic characterization of H9N2 swine influenza viruses in China. J. Gen. Virol. **88**:2035-2041.
19. **Butt AM, Siddique S, Idrees M, Tong Y.** 2010. Avian influenza A (H9N2):

computational molecular analysis and phylogenetic characterization of viral surface proteins isolated between 1997 and 2009 from the human population. Virol. J. **7**:319.

20. **Roberts NJ, Jr., Nichols JE.** 1989. Regulation of lymphocyte proliferation after influenza virus infection of human mononuclear leukocytes. J. Med. Virol. **27**:179-187.
21. **Tumpey TM, Lu X, Morken T, Zaki SR, Katz JM.** 2000. Depletion of lymphocytes and diminished cytokine production in mice infected with a highly virulent influenza A (H5N1) virus isolated from humans. J. Virol. **74**:6105-6116.
22. **Chanturiya AN, Basanez G, Schubert U, Henklein P, Yewdell JW, Zimmerberg J.** 2004. PB1-F2, an influenza A virus-encoded proapoptotic mitochondrial protein, creates variably sized pores in planar lipid membranes. J. Virol. **78**:6304-6312.
23. **Morris SJ, Price GE, Barnett JM, Hiscox SA, Smith H, Sweet C.** 1999. Role of neuraminidase in influenza virus-induced apoptosis. J. Gen. Virol. **80** (Pt 1):137-146.
24. **Zhirnov OP, Ksenofontov AL, Kuzmina SG, Klenk HD.** 2002. Interaction of influenza A virus M1 matrix protein with caspases. Biochemistry (Mosc) **67**:534-539.
25. **Zhirnov OP, Konakova TE, Wolff T, Klenk HD.** 2002. NS1 protein of influenza A virus down-regulates apoptosis. J. Virol. **76**:1617-1625.
26. **Chen W, Calvo PA, Malide D, Gibbs J, Schubert U, Bacik I, Basta S, O'Neill R, Schickli J, Palese P, Henklein P, Bennink JR, Yewdell JW.** 2001. A novel influenza A virus mitochondrial protein that induces cell death. Nat. Med. **7**:1306-1312.
27. **Bermejo-Martin JF, Martin-Loeches I, Rello J, Antón A, Almansa R, Xu L, Lopez-Campos G, Pumarola T, Ran L, Ramirez P.** 2010. Host adaptive immunity deficiency in severe pandemic influenza. Crit. Care. **14**:R167.
28. **Hagau N, Slavcovici A, Gonganau DN, Oltean S, Dirzu DS, Brezoszki ES, Maxim M, Ciuce C, Mlesnite M, Gavrus RL.** 2010. Clinical aspects and cytokine response in severe H1N1 influenza A virus infection. Crit. Care. **14**:R203.
29. **Lam WY, Yeung A, Chu I, Chan P.** 2010. Profiles of cytokine and chemokine gene expression in human pulmonary epithelial cells induced by human and avian influenza viruses. Virol. J. **7**:344.
30. **Perrone LA, Plowden JK, García-Sastre A, Katz JM, Tumpey TM.** 2008. H5N1 and 1918 pandemic influenza virus infection results in early and excessive infiltration of macrophages and neutrophils in the lungs of mice. PLoS. Pathog. **4**:e1000115.
31. **Li C, Hatta M, Watanabe S, Neumann G, Kawaoka Y.** 2008. Compatibility among polymerase subunit proteins is a restricting factor in reassortment between equine H7N7 and human H3N2 influenza viruses. J. Virol. **82**:11880-11888.

32. **Leung BW, Chen H, Brownlee GG.** 2010. Correlation between polymerase activity and pathogenicity in two duck H5N1 influenza viruses suggests that the polymerase contributes to pathogenicity. Virology **401**:96-106.
33. **Li C, Hatta M, Nidom CA, Muramoto Y, Watanabe S, Neumann G, Kawaoka Y.** 2010. Reassortment between avian H5N1 and human H3N2 influenza viruses creates hybrid viruses with substantial virulence. Proc. Natl. Acad. Sci . U. S .A. **107**:4687-4692.
34. **Huarte M, Falcon A, Nakaya Y, Ortin J, Garcia-Sastre A, Nieto A.** 2003. Threonine 157 of influenza virus PA polymerase subunit modulates RNA replication in infectious viruses. J. Virol. **77**:6007-6013.
35. **Song J, Feng H, Xu J, Zhao D, Shi J, Li Y, Deng G, Jiang Y, Li X, Zhu P, Guan Y, Bu Z, Kawaoka Y, Chen H.** 2011. The PA protein directly contributes to the virulence of H5N1 avian influenza viruses in domestic ducks. J. Virol. **85**:2180-2188.
36. **Hu J, Hu Z, Mo Y, Wu Q, Cui Z, Duan Z, Huang J, Chen H, Chen Y, Gu M, Wang X, Hu S, Liu H, Liu W, Liu X.** 2013. The PA and HA gene-mediated high viral load and intense innate immune response in the brain contribute to the high pathogenicity of H5N1 avian influenza virus in mallard ducks. J. Virol. **87:**11063-11075.
37. **Desmet EA, Bussey KA, Stone R, Takimoto T.** 2013. Identification of the N-Terminal Domain of the Influenza Virus PA Responsible for the Suppression of Host Protein Synthesis. J. Virol. **87**:3108-3118.
38. **Gabriel G, Herwig A, Klenk HD.** 2008. Interaction of polymerase subunit PB2 and NP with importin alpha1 is a determinant of host range of influenza A virus. PLoS. Pathog. **4**:e11.
39. **Gu J, Xie Z, Gao Z, Liu J, Korteweg C, Ye J, Lau LT, Lu J, Zhang B, McNutt MA, Lu M, Anderson VM, Gong E, Yu AC, Lipkin WI.** 2007. H5N1 infection of the respiratory tract and beyond: a molecular pathology study. Lancet **370**:1137-1145.
40. **Sun Y, Qin K, Wang J, Pu J, Tang Q, Hu Y, Bi Y, Zhao X, Yang H, Shu Y.** 2011. High genetic compatibility and increased pathogenicity of reassortants derived from avian H9N2 and pandemic H1N1/2009 influenza viruses. Proc. Natl. Acad. Sci . U. S .A. **108**:4164-4169.
41. **Reed LJ, Muench H.** 1938. A simple method of estimating fifty per cent endpoints. Am. J. Epidemiol. **27**:493-497.

Figure legends

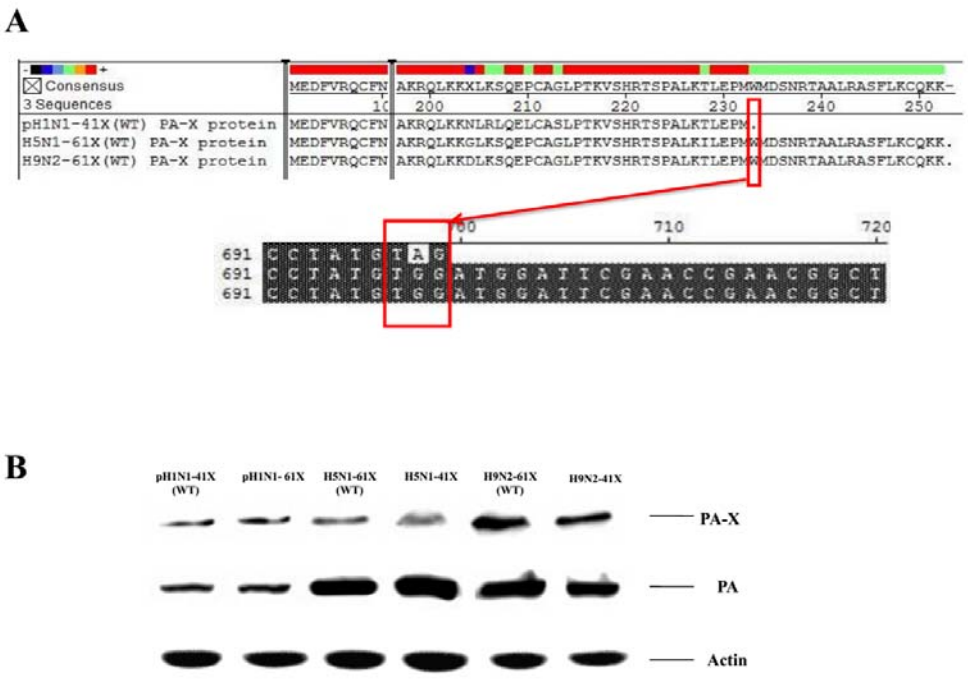

Figure 1. PA-X and PA sequences of viruses used in this study. (A) Sequences of the C-terminal regions of PA-X proteins of several epidemiologically important strains. (B) Western blot analysis for the detection of PA-X protein in MDCK cells infected with pH1N1, H5N1, and H9N2 mutant viruses.

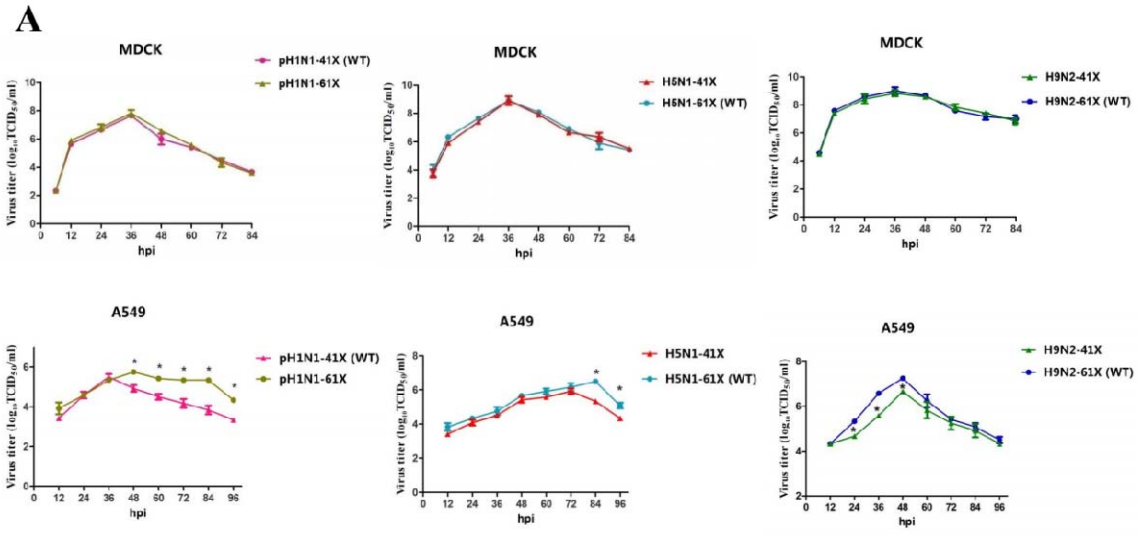

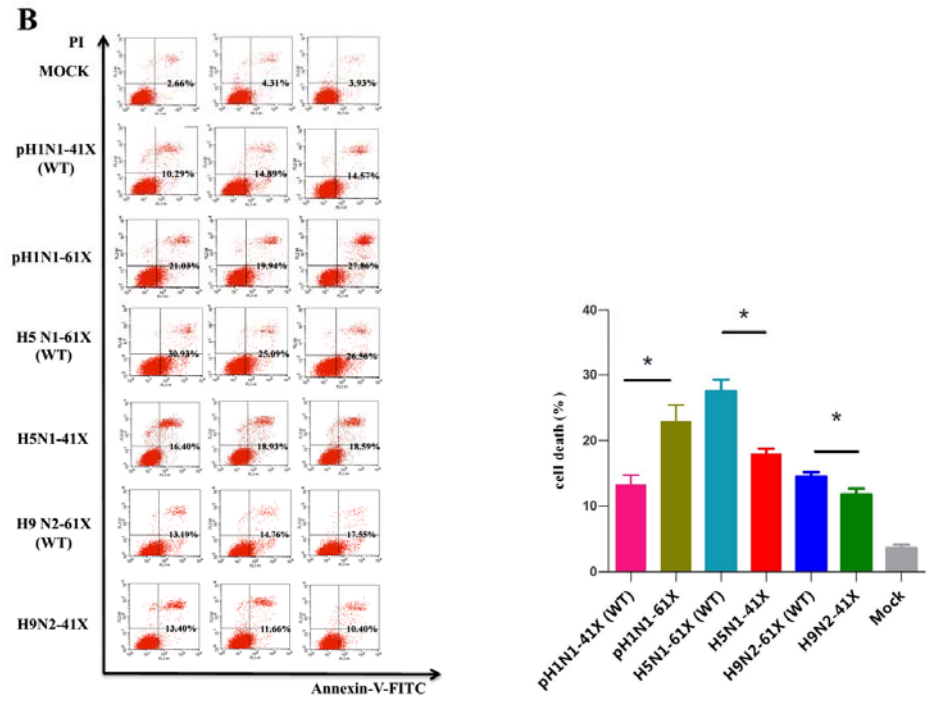

Figure 2. pH1N1, H5N1, and H9N2 viruses with full-length PA-X showed more replication and apoptosis in A549 cells. (A) Viral growth curves of pH1N1, H5N1. and H9N2 mutant viruses in MDCK cells and A549 cells over 84 and 96 h. Each value represents the mean of three independent experiments performed in triplicate; error bars indicate standard deviations. (B) Relative induction of cell death as determined by the detection of annexin^{+} and PI^{+} A549 cells infected with the indicated panel of viruses at a 1.0 MOI for 12 h. Representative dual-labeled quadrants of

596 bivariant fluorescence dot plots show the relative induction of apoptosis (annexin^{+})
597 and necrosis (PI^{+}) in infected cells. Apoptotic cells that were positive for annexin V
598 but not PI are shown in the right lower quadrant, and those positive for PI but not
599 annexin V are shown in the left upper quadrant. Percentages shown are proportions of
600 apoptotic cells. Mock, uninfected control cells. * indicates significant differences
601 between pH1N1-61X and pH1N1-41X (WT), H5N1-41X and H5N1-61X (WT), and
602 H9N2-41X and H9N2-61X (WT).
603

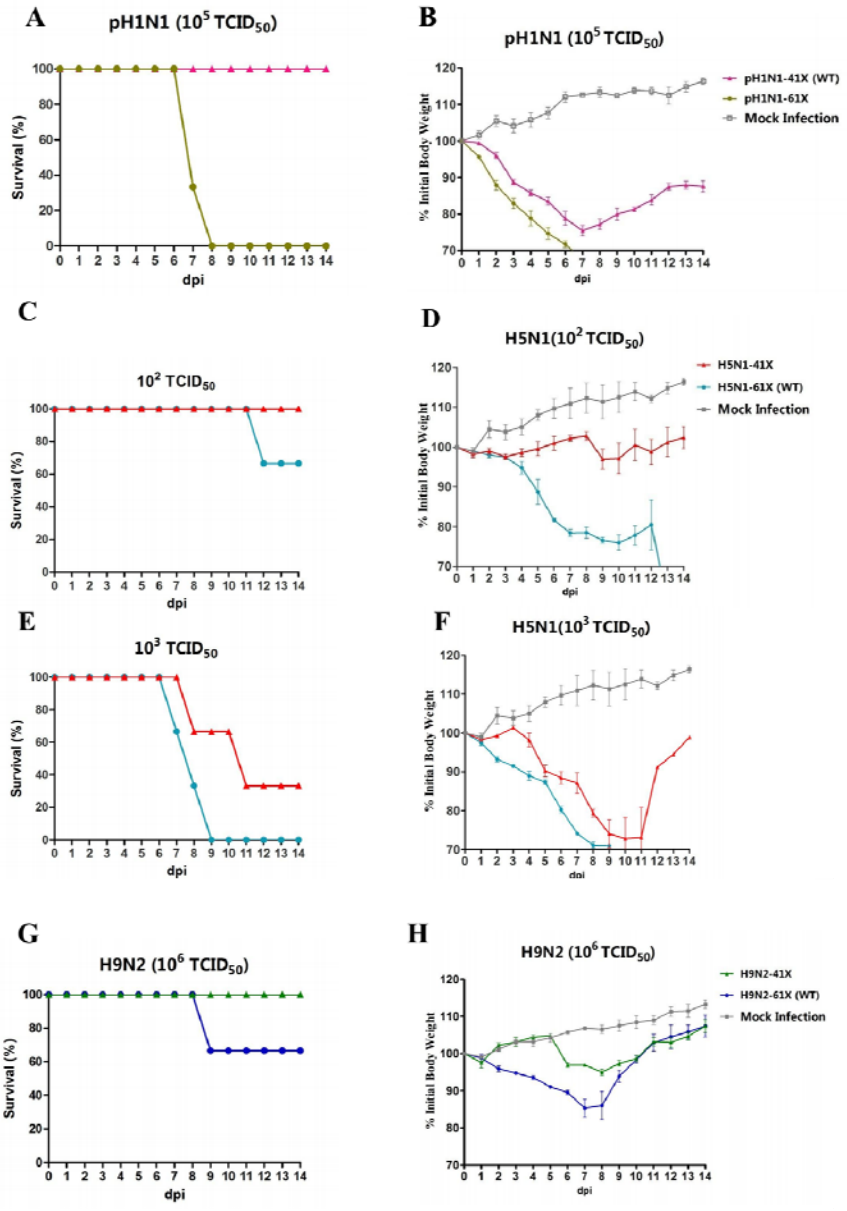

Figure 3. Mortality and weight loss in mice intranasally inoculated with PA-X mutant viruses. The data show the survival (percentage) of mice infected with (A) pH1N1 PA-X, (C&E) H5N1 PA-X, and (G) H9N2 PA-X mutant viruses. The body weight of mice inoculated with (B) pH1N1 PA-X, (D&F) H5N1 PA-X, and (H) H9N2 PA-X mutant viruses was presented as percentage of the weight on the day of inoculation (day 0). Any mouse that lost more than 30% of its body weight was euthanized. The means of each group are shown, and error bars are standard deviations (SDs).

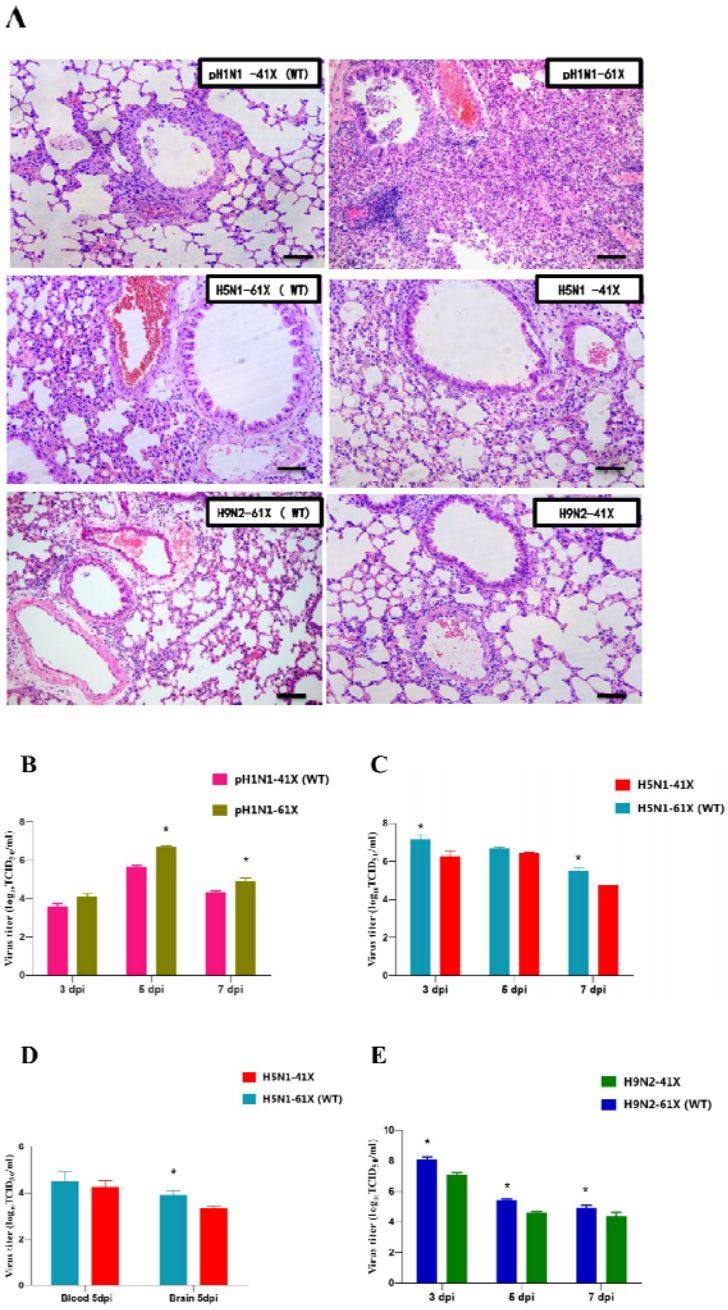

Figure 4. (A) Histopathological changes and (B, C, D, E) viral titers in lungs of mice infected with pH1N1, H5N1, and H9N2 mutant viruses. Scale bars, 100 μm. The mean viral lung load ± SD was calculated by $\log_{10}$ $TCID_{50}$ determination in MDCK cells. * indicates significant difference between pH1N1-61X and pH1N1-41X (WT), H5N1-61X (WT) and H5N1-41X, and H9N2-61X (WT) and H9N2-41X.

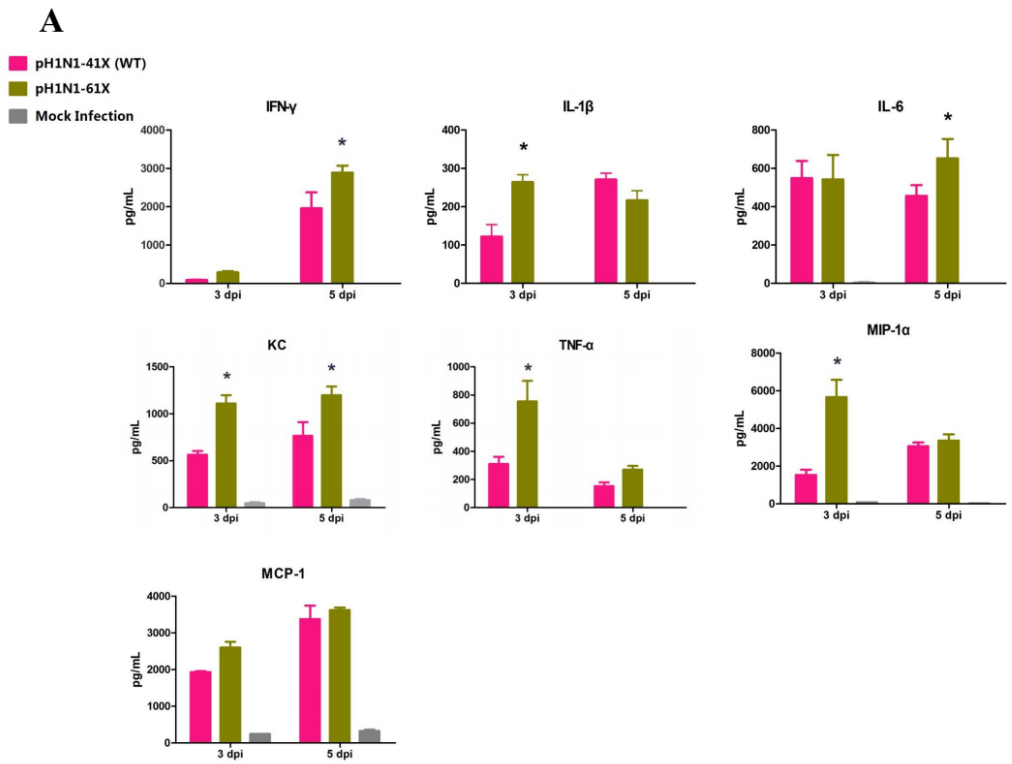
A
pH1N1-41X (WT)
pH1N1-61X
Mock Infection
IFN-γ
IL-1β
IL-6
KC
TNF-α
MIP-1α
MCP-1
pg/mL
3 dpi
5 dpi

621

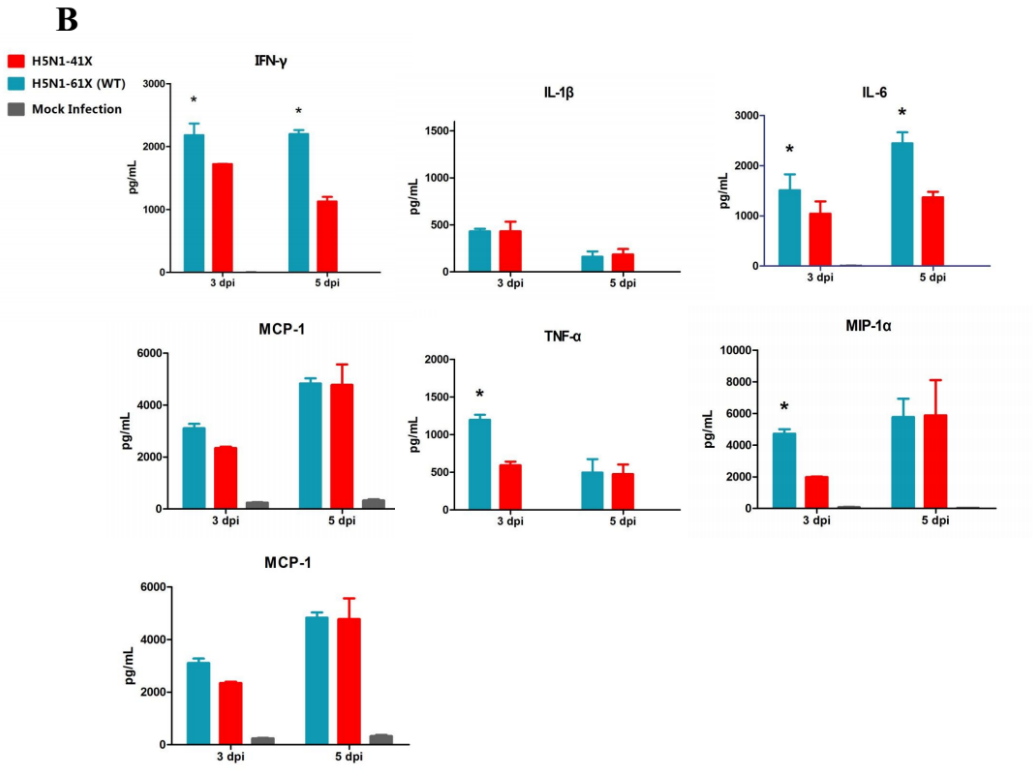
B
H5N1-41X
H5N1-61X (WT)
Mock Infection
IFN-γ
IL-1β
IL-6
MCP-1
TNF-α
MIP-1α
MCP-1
pg/mL
3 dpi
5 dpi

622

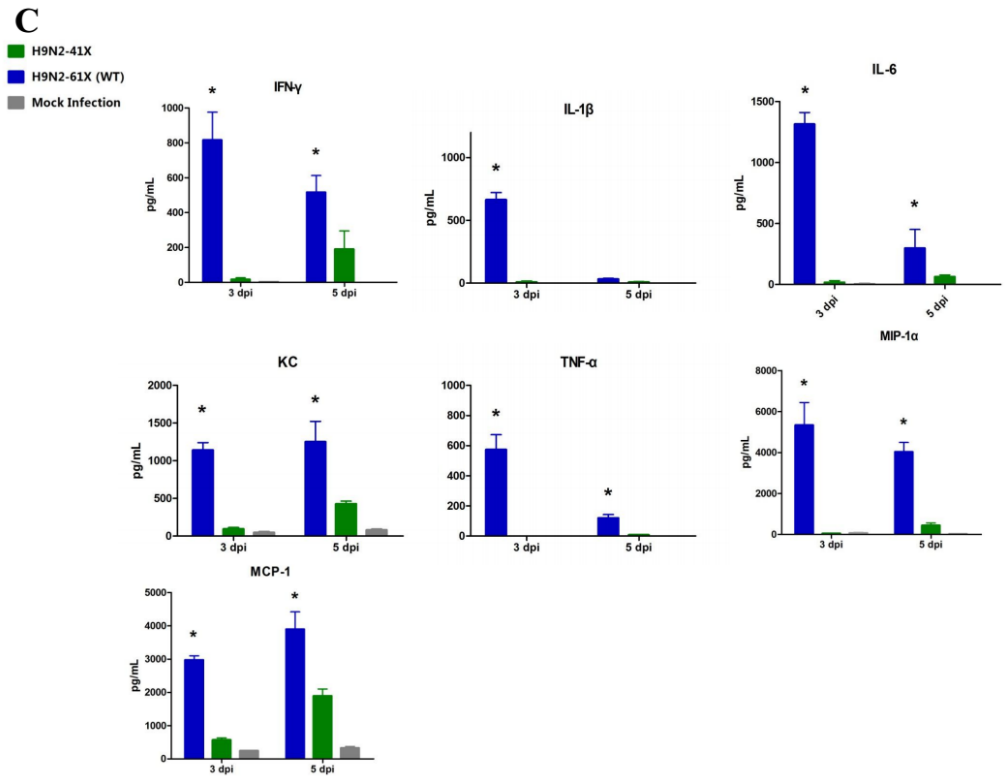

Figure 5. Detection of cytokine and chemokine proteins in lungs of mice infected with (A) pH1N1, (B) H5N1, and (C) H9N2 PA-X mutant viruses. Mean cytokine/chemokine levels ± SD are shown. * indicates significant differences between viruses with full length PA-X and truncated PA-X.

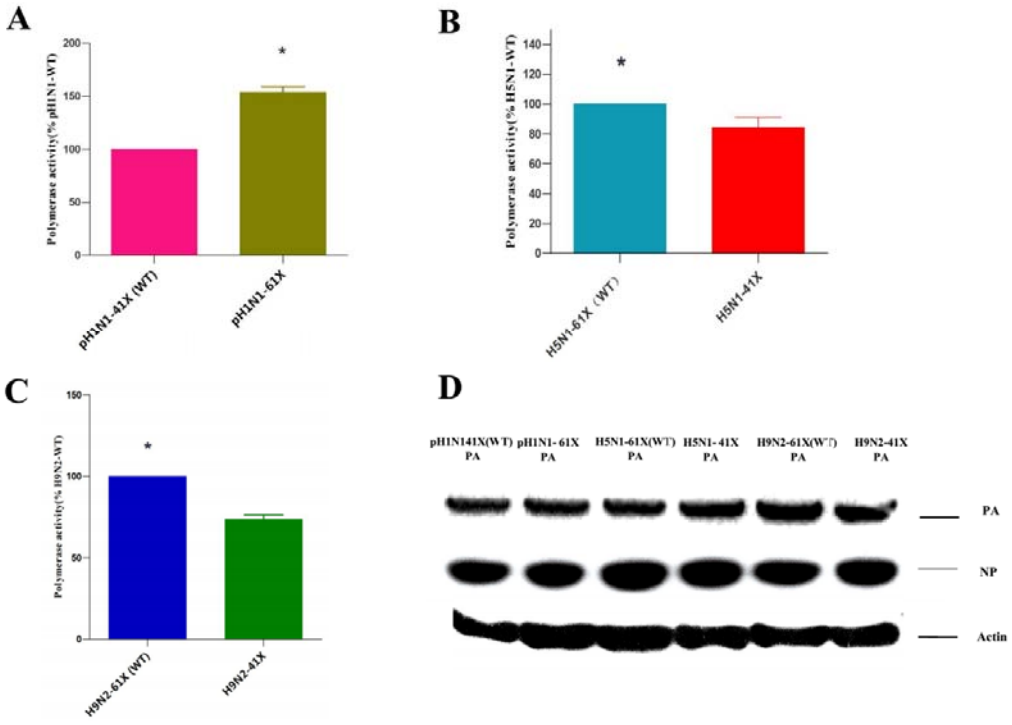

Figure 6. Full-length PA-X showed considerable viral polymerase activity. (A) Polymerase activity of (A) pH1N1, (B) H5N1, and (C) and H9N2 viruses with full-length PA-X and truncated PA-X, expressed as mean activity ± SD relative to corresponding wild-type PA set at 100% from three independent experiments. (D) Western blot detections of PA, NP, and β-actin in protein lysates from 293T cells transfected with polymerase plasmids. * indicates significant differences between pH1N1-61X and pH1N1-41X (WT), H5N1-61X (WT) and H5N1-41X, and H9N2-61X (WT) and H9N2-41X.

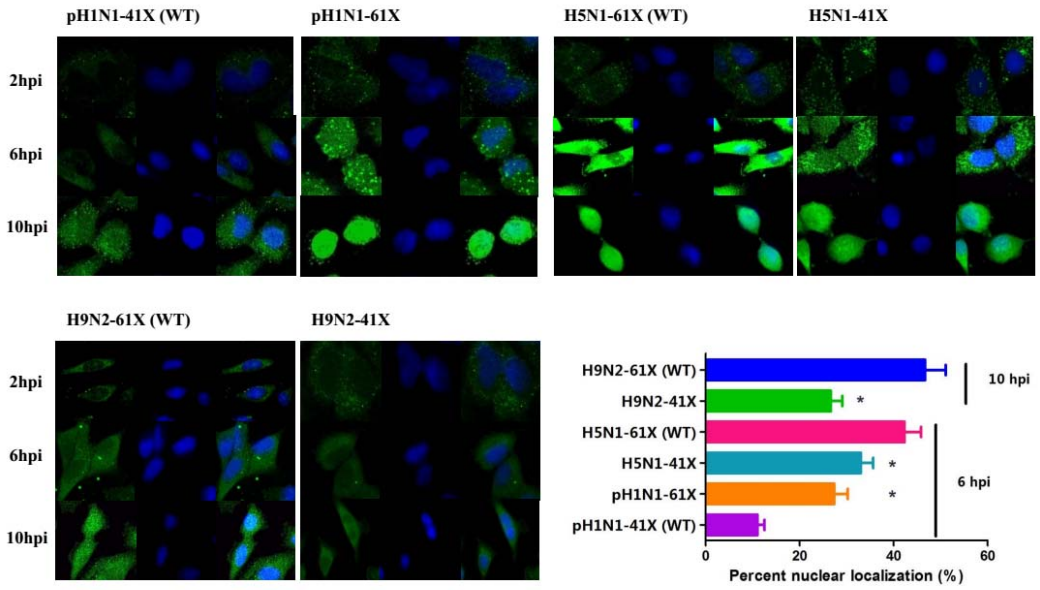

639

640 **Figure 7. Nuclear transport of PA proteins with full-length and truncated PA-X**
641 **in infected cells.** (A) PA protein in A549 cells infected with pH1N1-61X,
642 pH1N1-41X (WT), H5N1-61X (WT), H5N1-41X, H9N2-61X (WT), and H9N2-41X
643 virus at 2.0 MOI was localized by immunofluorescence at 2, 6, and 10 hpi. Nuclei
644 were stained with DAPI. (B) At 6 hpi and 10 dpi, nuclear PA quantification was based
645 on proportion of infected cells (n=100) with clear nuclear presence of PA. Values
646 shown are means of the results of three independent experiments ± SDs. *, $P < 0.05$
647 relative to cells infected with corresponding wild-type viruses.

648

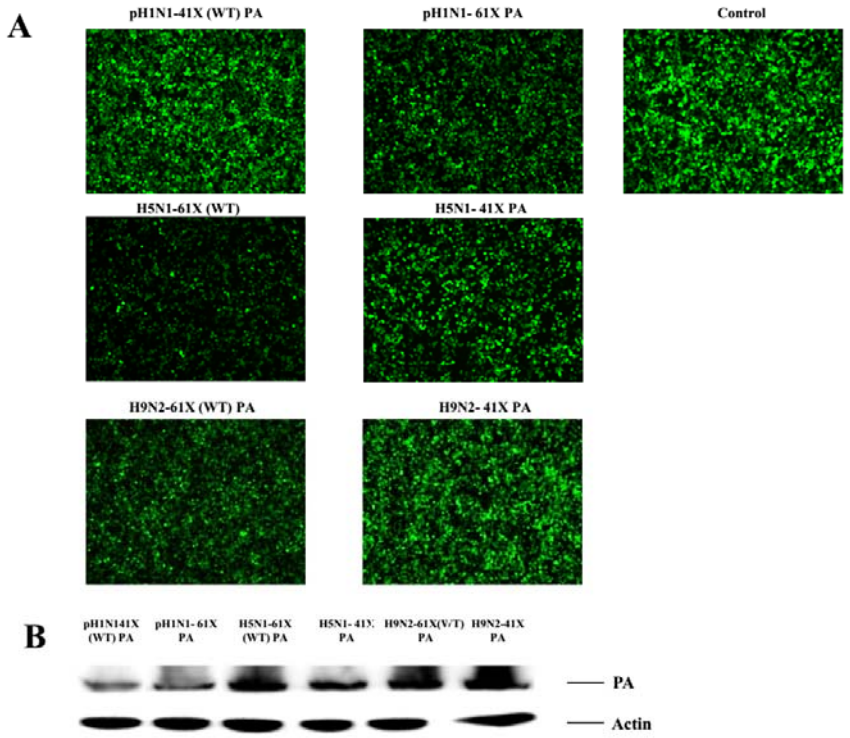

649

650 **Figure 8. PAs were more effective in suppressing non-viral protein synthesis with**
651 **full length PA-X than with truncated.** (A) 293T cells were co-transfected with eGFP
652 expression plasmid and PA plasmids with full-length or truncated PA-X from pH1N1,
653 H5N1, and H9N2 viruses. (A) Fluorescence images indicative of eGFP expression at
654 24 h after transfection were captured under identical exposure conditions. (B) PA
655 protein was determined using Western blotting and anti-PA antibody. Anti-β-actin
656 antibody was used as a loading control. Control was 293T cells co-transfected with
657 eGFP expression plasmid and empty pcDNA3.1 vector.